INL/CON-12-26395
PREPRINT

On Techniques to Characterize and Correlate Grain Size, Grain Boundary Orientation and the Strength of the SiC Layer of TRISO Coated Particles: A Preliminary Study

HTR 2012

I. J. van Rooyen
M. L. Dunzik-Gougar
P. M. van Rooyen
T. Trowbridge

October 2012

The INL is a
U.S. Department of Energy
National Laboratory
operated by
Battelle Energy Alliance

Proceedings of the HTR 2012
Tokyo, Japan, October 28 – November 1, 2012
Paper HTR2012-3-024

On Techniques to Characterize and Correlate Grain Size, Grain Boundary Orientation and the Strength of the SiC Layer of TRISO Coated Particles: A Preliminary Study

IJ van Rooyen[1], ML Dunzik-Gougar[1,2], PM van Rooyen[3], T Trowbridge[1]
[1]Idaho National Laboratory
Idaho Falls, ID 83415-6188, USA
phone: +1-208-5337199, isabella.vanrooyen@inl.gov

[2]Department of Nuclear Engineering, Idaho State University, Idaho Falls, ID 83402, USA

[3]Philip M van Rooyen Network Consultants, Midlands Estates, South Africa

Abstract – *The mechanical properties of the silicon carbide (SiC) layer of the TRi-ISOtropic (TRISO) coated particle for high temperature gas reactors (HTGR) are among the most important parameters that determine fuel performance. Measuring techniques thereof are not standardized in the international VHTR community. In addition, the effect of temperature on these mechanical properties has not been correlated with grain characteristics. Grain characteristics are known to be temperature dependent and a greater understanding of this phenomenon may contribute to answering questions about Ag transport through the SiC layer. This paper integrates and compares results obtained from two different types of strength measurements namely the modified compression test and nano indentation hardness as a function of temperature. The effect of annealing temperature in the range of 1000 to 2100˚C are evaluated, because these temperatures are relevant to potential safety margin-related questions at accident conditions as well as possible future design criteria for higher temperature applications. Also explored are possible relationships between the average grain size and strength values. Grain sizes determined using the Lineal intercept method are compared with results obtained by electron backscatter diffraction (EBSD) technique. Preliminary grain boundary characterization results via EBSD are included along with a brief discussion of the effects of sample preparation techniques (eg FIB) and relative location on the sample. These results are also important for future fission product transport studies, as grain boundary diffusion is identified as a possible mechanism by which ^{110m}Ag, one of the fission activation products, might be released through intact SiC layers. Recommendations and future work are also briefly discussed.*

I. INTRODUCTION

A significant challenge for next generation, high temperature nuclear reactor designs is the availability of new materials compatible with the extreme conditions. Development of such a material is the focus of work presented here. Silicon carbide (SiC) has extraordinary thermomechanical and physiochemical properties, including chemical stability, thermal and radiation resistance, high resistance to oxidation, high thermal conductivity and high mechanical strength. The dimensional stability under high temperature (maximum linear expansion of 0.7 % at 250 °C) and irradiation conditions further make SiC a material of interest. Of greatest significance for the nuclear industry, SiC serves as the main barrier to fission product (FP) release in the high temperature gas-cooled reactor fuels.

TRi-ISOstructural (TRISO) coated particle fuel incorporates a SiC layer designed to withstand the pressures of fission and transmutation product gases in a high temperature and

radiation environment. Performance of this vital SiC layer is a function of many factors, including manufacturing parameters and reactor operating conditions. Correlations among these factors and SiC properties may be quantifiable, thereby allowing prediction of particle performance based on measurements of a few basic properties such as hardness, strength and grain size, rather than extensive characterization. The techniques used and/or developed for these measurements, focusing on eliminating artificial contributions due to sample preparation and ease of measurements in the fabrication environment.

Previous publications by the authors presented results of studies correlating layer thickness and annealing temperature with the strength and hardness of the SiC [1, 2, 3]. In this paper, results of the influence of annealing temperature on strength, hardness and grain size is evaluated. In addition, preliminary results of current research on grain boundary characteristics (orientation and size) of CVD SiC in TRISO fuel particles are presented.

Initial work on the effect of temperature on the grain size was reported by Van Rooyen *et al.* [4]. Although the maximum normal operating temperature of a VHTR reactor design is in the region of 1000°C, the temperature may reach 1600°C during accident conditions and therefore annealing temperatures from 1000 – 2100 °C were chosen for the original studies. In addition these results may contribute towards the increase of the safety margin for using TRISO coated particles at higher temperature conditions in new reactor designs. Long duration annealing (>100h) studies, although important for the effect on SiC strength as it is an indication of how the grain size will be modified during the reactor operation under specific conditions, was only partially addressed by previous work done by the authors.

II. MATERIALS AND METHODS

Coated particles used in this study (as well as the others previously mentioned) have ZrO_2 surrogate kernels surrounded consecutively by layers of carbon buffer, (inner) pyrolytic carbon (IPyC), SiC, and (outer) pyrolytic carbon (OPyC). The SiC layer was applied via chemical vapor deposition at various combinations of temperature and deposition rate in one of two coaters. The Research Coating Facility (RCF) and the Advanced Coating Facility (ACF) at the South African Nuclear Energy Corporation (NECSA) differ in their capacity (1kg and 5kg, respectively) and in the SiC deposition rate (see Table 1). Particles were categorized into batches as shown in Table 1.

Batch & Coater	SiC		Outer PyC	
	Selected Coating Parameters	Layer thickness (µm)	Selected Coating Parameters	Layer thickness (µm)
A (ACF)	1510°C Rate not available	32	1300°C Rate not available	39
B (RCF)	1510°C Rate 0.17µm/min	30	1300°C Rate 2.12µm/min	32
C (RCF)	1585°C Rate 0.17µm/min	30	1300°C Rate 0.45µm/min	9
D (ACF)	1450°C Rate 0.23µm/min	39	1280°C Rate 5.65µm/min	48
E (ACF)	1510°C Rate 0.24µm/min	32	1300°C Rate 5.65µm/min	48

Table 1: Selected coated particle fabrication conditions.

After production, coated particles from each batch were annealed at a temperature in the range 1000°C-2100°C for 10 minutes to 100 hours as summarized in Table 2.

Post-Production Annealing Parameters	
Temperature (°C)	Time (min)
1000	60
1300	60
1500	60
1600	60 and 6000
1700	60
1800	60
1900	60
1980	60
2000	30
2100	10

Table 2: Coated particle post-production annealing conditions.

Fracture strength of the coated particle SiC layer was determined with a modified compressive strength method developed and reported by Van Rooyen *et al.* [2]. Coated particles were compressed between soft anvils and Finite Element Analysis modeling was used to quantify the stress to which the particle was subjected. Average strength, characteristic strength and the Weibull modulus were also determined [2]. The number of coated particles

tested to obtain these results is summarized in Table 3 and is in more detail described in [2].

CP Batch	Number of compression test samples tested after post-fabrication annealing (Temperature °C)				
	25	1600	1800	2000	2100
A	30	30	No data	29	7
B	31	31	No data	No data	22
C	31	31	No data	No data	20
D	102	25	31	100	No data
E	102	31	31	31	No data

Table 3: Summary of number of coated particles tested for each batch using the compression fracture test.

Hardness of the SiC layer was measured with a CSM Nano-indentation Hardness tester on polished cross sectioned pieces to the equator of the coated particles, applying a load of 100 mN maintained for 15 seconds before unloading. The nano hardness measurements for all batches were done on one particle but at three different positions and a total of 27 measurements per batch were measured. Earlier work by Van Rooyen *et al*. [5] showed that this method provides representative measurements. The work presented in this paper is based on the average values of the results obtained and the detail of the measurements are described by Van Rooyen *et al*. [5].

As described in [3], grain size (diameter) determination was carried out using the Heyns Lineal Intercept procedure in accordance with ASTM E112-96 (2004) [6]. To produce more accurate grain size (area) measurements and gather information about grain boundary orientation, samples are currently undergoing analysis via electron backscatter diffraction (EBSD) [7, 8].

The analysis of the prepared samples was done using an EDAX TSL Hikari electron backscattered detector coupled to a FEI Quanta FEG650 scanning electron microscope. The sample was tilted at 70° within the chamber with fine calibration of the detector geometry using the crystal structure for 3C-SiC, the SiC polytype expected to be present. The area for the EBSD analysis was selected with a step size of 50 nm initially for the first measurement and then standardized at 0.1 µm for the mapping chosen for the second and third analyses. For each scan, the duration was typically between 3 to 4 h. The scan size was approximately 13 µm x 36 µm. It is however noted that the field of EBSD analyses during this preliminary study was very small due to the initial difficulty in sample preparation and it is recommended for future work that the field be enlarged to approximately 50 µm x 35 µm.

III. RESULTS AND ANALYSIS

III.A. Property and Parameter Correlations

Table 4 provides a summary of the physical measurements (hardness, size and strength) obtained on coated particles from each batch. Particles that were not annealed post-production, (i.e. maintained at room temperature (~25°C)), serve as reference particles for comparison to those annealed at one of four temperatures for 1 hour at 1600°C and 1800°C, and for 30 min and 10 min at 2000°C and 2100°C, respectively.

CP Batch	Post-Production Annealing Temperature (°C)				
	25	1600	1800	2000	2100
A	N, S	N, S	No data	N, S	N, S
B	N, S	N, S	No data	N	N, S
C	N, S	N, S	No data	N	N, S
D	N, S, G	S, G	N, S, G	N, S, G	No data
E	N, S, G EBSD	S, G	N, S, G	N, S, G	No data
N	Nano-indentation Hardness [MPa]				
G	Grain Size [µm] (Lineal Intercept method)				
S	Characteristic Strength [MPa]				

Table 4: Summary of physical property measurements for coated particle batches.

Each data set (e.g., the set of data comprising the nano-indentation hardness measurements for coated particles from batch A annealed at 1600°C) in which 3 or more values exist was compared to another property of the same particles. As such, eligible data were identified and analyzed as follows:

- Grain size vs. hardness and grain size vs. strength for Batches D & E
- Hardness vs. strength for all batches annealed at 25 and 1600 °C

The pairs of properties were analyzed for linear correlation via least squares fit. In the data plots, the straight line least squares fit is denoted with an asterisk (*) next to the batch name. The variability of the data with respect to the least squares fit is presented as the coefficient of determination, R^2. The goodness of the least squares fit is given by the Significance Factor of the regression analysis calculation, According to [9] values for the Significance Factor smaller than 0.05 indicates that the correlation between the properties are significant. The data sets of the

pairs of properties that are used to calculate the correlations consist of 3, 4 and 5 data points only. These are very small data sets. The values of the Significant Factors for the calculated correlations range from 0.133 to 0.783 which indicates mild to no correlation between the parameters. These values of the Significance Factors explain the range of R^2 values that is between 0.933 and 0.051. To be able to define a significant correlation between parameters more data points are needed. Completing the measurements of Table 4 will give the maximum data points possible which can be used to determine if there are significant correlations between the properties.

III.A.1 Grain Size vs. Hardness and Strength

Figure 1 presents the comparison of properties measured for coated particles from batches D and E. Trends seen in Figures 1 and 2 suggest sensitivity to the measurement techniques. It is expected that nano indentation hardness and strength would vary similarly with grain size; however, opposite trends are seen. The next step in these data analyses is to determine the theoretical (physics) relation between the two measurements and grain sizes. In addition, it is further recommended that the yield strength of the nano indentation results also be evaluated for possible trends. Recent work by Miura *et al.* [10] indicated that the orientation of grains also have an influence on the hardness and nano indentation values. This may offer a reason for the behavior observed as mentioned above. More complete EBSD characterization to establish the surface grain orientation would help confirm this hypothesis.

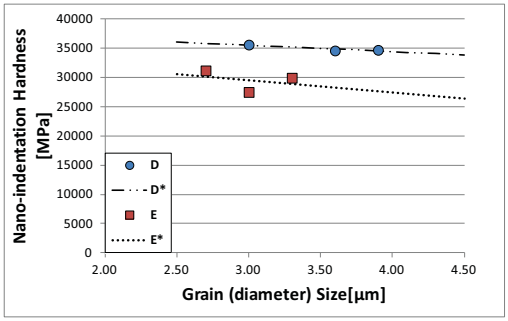

Figure 1: Comparison of SiC layer grain size and hardness for Batches D & E coated particles [R^2(D) = 0.83 and R^2(E) = 0.11].

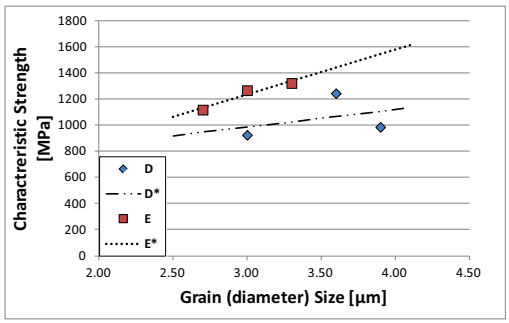

Figure 2: Comparison of SiC layer grain size and strength for Batches D & E coated particles [R^2(D) = 0.13 and R^2(E) = 0.93].

III.A.2 Hardness vs. Strength

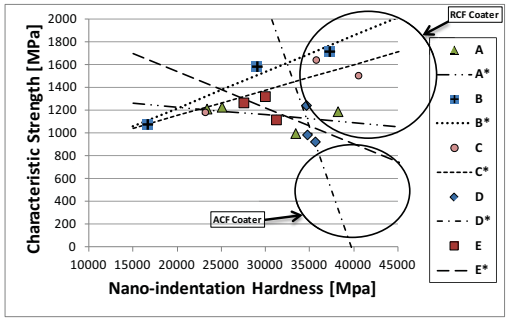

Figure 3: Comparison of SiC layer hardness and strength as functions of coater facility for Batches A - E coated particles [R^2(A) = 0.20, R^2(B) = 0.96, R^2(C) = 0.71, R^2(D) = 0.52, R^2(E) = 0.32].

From Figure 3 it is clear that correlations between SiC layer hardness and strength are a function of the CVD coater. SiC layers created with the RCF coater have strengths directly related (i.e. the least squares fit line has a positive slope) to the hardness values. Correlations between the values for the three ACF coater batches are significantly weaker, with R^2 values of 0.2, 0.5 and 0.3, respectively. The negative slopes of the least squares fit lines indicate an indirect relationship between hardness and strength for these coated particles. Further, though all slopes are negative, they differ significantly from each other, making it impossible to establish generic behavior.

There appear to be no correlations between hardness and strength when grouped according to annealing temperature; however, Figure 4 reinforces the influence of CVD coater on the physical properties seen in Figure 3. All tested particles coated in the RCF are stronger than their annealing temperature counter parts coated in the

ACF. This phenomenon has been discussed in an earlier publication [2].

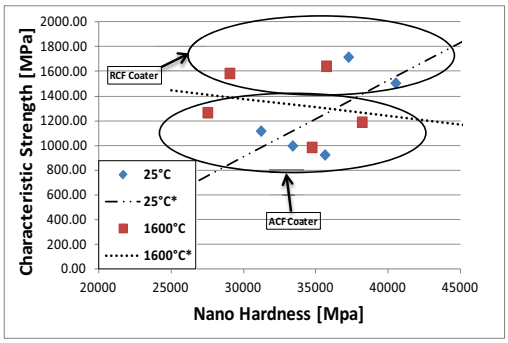

Figure 4: Comparison of SiC layer hardness and strength as functions of annealing temperature for Batches A - E coated particles [R^2(25°C) = 0.42 and R^2(1600°C) = 0.05].

III.B. Grain size and grain boundary characteristics

III.B.1 Methods and Sample preparation

Measurements of SiC grain size with EBSD analysis offers significant advantages to the Lineal Intercept method that was used in the original studies. The Lineal intercept method is plagued by sample preparation issues resulting in uneven etching and rounding of grain edges. Further, it requires differentiation between stacking faults and grain boundaries with the naked eye. Micrographs of coated particles from Batch E shown in Figures 5 and 6 provide clear examples of the complicating effects of sample preparation.

The average SiC grain size can be determined using the area weighted average of grains in an EBSD image, as described by Kirchover [11]. This method offers the advantage that the influence of the small un-indexable points – points that could not be recognized by EBSD software – is diminished because the area of these points is negligible. Even if there are a significant number of these points compared to the large grains populating the SiC layer, the area is statistically insignificant. Prior to the analysis the data are filtered to remove points with low confidence index. Most such points correspond to the SiC layer boundaries with pyrolytic carbon and a few correspond to grain boundaries. The detailed description of the EBSD technique is given in [12].

Grain boundary characteristics measurement using EBSD technique is very sensitive of sample preparation as a very flat smooth layer is needed to enable good patterns. Various sample techniques are available and used successfully for various materials, but the polishing techniques used for coated particle cross sections, pose unique challenges due to the different removal rates at SiC-IPyC interfaces. This results in the rounding effect of the SiC if increased polishing time is used to obtain the required bulk SiC surface finish. However, good flat surfaces were obtained and used for three datasets reported in section *111.B2*. In addition to this method, an additional preparation technique was used to prepare an oversized TEM sample using FIB as a machining tool. This method provided a very smooth and flat surface over the whole SiC layer area and is discussed in section *111. B5*. Detailed description of this sample preparation technique will be reported elsewhere.

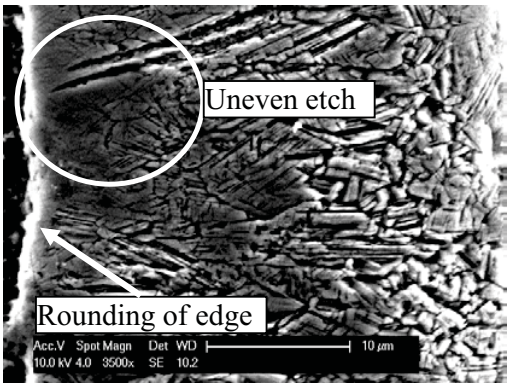

Figure 5: Micrograph of SiC layer for non-annealed coated particle from Batch E (average grain diameter 2.7 µm).

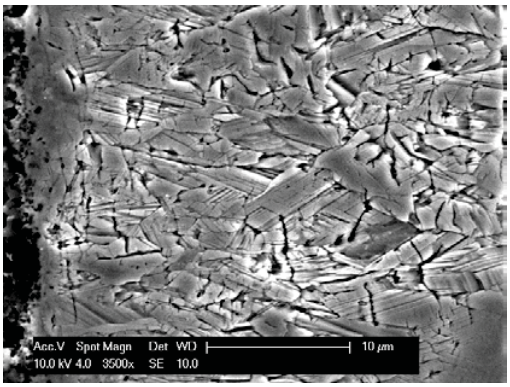

Figure 6: Micrograph of SiC layer for coated particle from Batch E annealed at 1600°C (average grain diameter 3 µm).

III.B.2 Location and representativeness of EBSD area

To determine the areal location to use for EBSD measurements, a study was completed on two coated particles from a specific batch namely the non –annealed batch E (also called E-ref). Due to the time required for sample preparation, often only one EBSD area is used. However, the results may vary depending on the homogeneity of the coated particle itself as well as the representativeness of the specific coated particle of the batch.

Cross-sections of the coating layers of two particles from the same batch (E) were analyzed via EBSD. For particles E1 and E2, Figure 7 presents the SiC grain diameter distribution based on weight averaged values with respect to the number fraction of grains having a given diameter. The second particle, E2, was characterized at two locations in the SiC layer to determine consistency within a given particle. No significant difference is observed when comparing the average grain sizes, suggesting that these ESBD-based grain size measurements are representative. The inverse pole figure key map is shown in Figure 8 and the grain orientation and size distribution are shown in Figures 9 to 11. No preferred orientation is observed either on the two edges or through the thickness of the SiC layer.

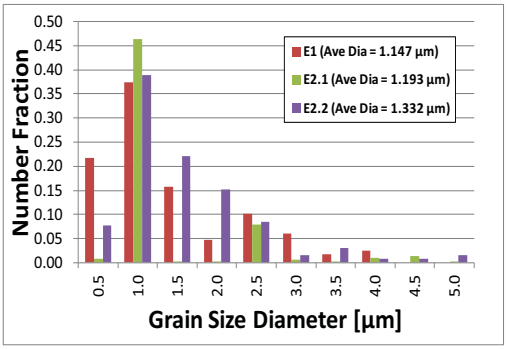

Figure 7: SiC layer grain size (diameter) distribution via EBSD analysis of a non-annealed coated particle E1 and particle E2, locations 1(E2.1) and 2 (E2.2).

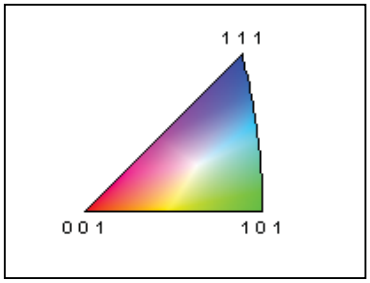

Figure 8: EBSD inverse pole figure key map

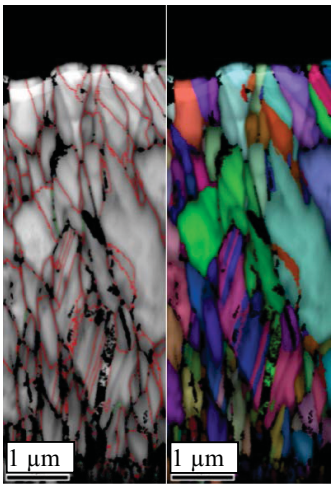

Figure 9: EBSD image of SiC layer grains in the non-annealed coated particle E1. The red overlay on the left side shows the high angle boundaries and the orientation is shown in the right hand side image.

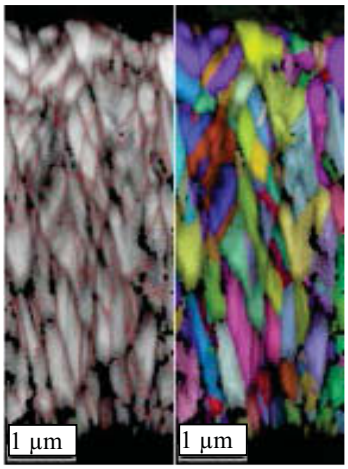

Figure 10: EBSD image of SiC layer grains at Location 1 of the non-annealed coated particle E2.1. The red overlay on the left side shows the high angle boundaries and the orientation is shown in the right hand side image.

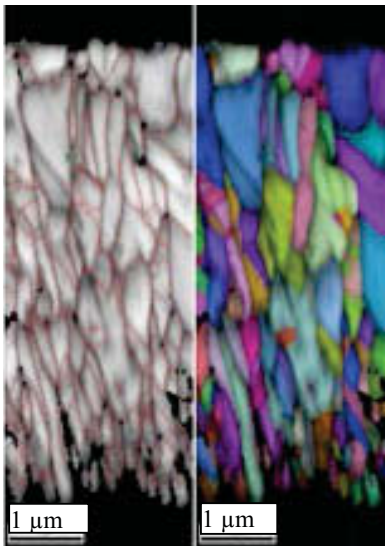

Figure 11: EBSD image of SiC layer grains at Location 2 of the non annealed coated particle E2.2. The red overlay on the left side shows the high angle boundaries and the orientation is shown in the right hand side image.

III.B.3 Grain Boundary Character Distribution via EBSD

In addition to determining the grain boundary size distribution for the characterized coated particles, the SiC grain boundary character was also studied. The grain boundary character distribution (GBCD) was determined in terms of the coincidence site lattice (CSL) model using the Brandon's criterion [13,14,15]. High-angle grain boundaries, low angle boundaries, and boundaries with significant lattice site coincidence (CSL) were mapped and their fractions determined.

A summary of the CSL grain boundaries for coated particles E1 and E2 are presented in Figure 12. The distribution of the high angle boundaries that are shown in red in Figures 9 to 11 and the misorientations angle distribution are shown in Figures 12 to 16 in pie chart form.

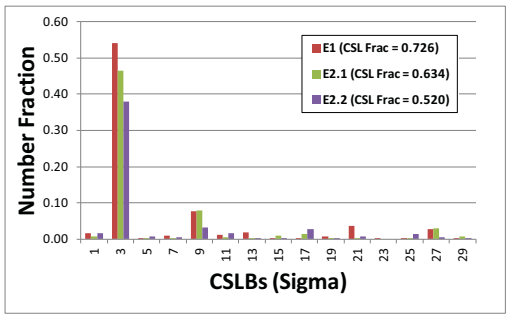

Figure 12: SiC layer CSL Boundary distribution comparison analysis of the non-annealed coated particle E1 and the non-annealed particle E2, locations 1 (E2.1) and 2 (E2.2).

Although the average grain size determined via EBSD analysis varied little among the three data sets, there does seem to be some variation in the grain boundary character distribution between these particles from a single batch and between locations on a single particle. If this preliminary observation is confirmed within more batches showing similarly variable GBCDs, the impact on coated particle characterization and qualification may be significant. This may be a possible reason why up until now, the Ag release through apparently similar SiC layers varied so widely. Previous studies have not had access to EBSD.

Kim *et al.* [14] have demonstrated via modeling that when grain orientation, texture, and grain size are fixed, macroscopic properties can still be affected by changes in the distribution of misorientations and grain boundary plane orientations. In other words, grain boundary character distribution may well be a sensitive metric of polycrystalline structure that can be related to macroscopic properties.

Other researchers [15] have linked GBCD and boundary energy. A large value for the fractional distribution of a given CSL correlates with a more stable bond, with low energy. This correlation implies an ability to predict macroscopic properties based on microscopic measurements. For example, in brittle materials the fracture strength is inversely proportional to the average bond energy density. Chemical properties, such as the rate of intergranular corrosion, have also been linked to GBCD [16].

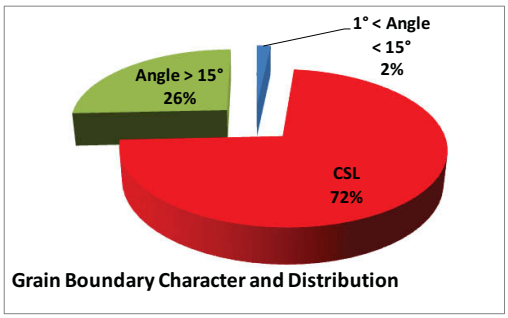

Figure 13: SiC layer grain boundary character distribution via EBSD analysis of the non-annealed coated particle E1.

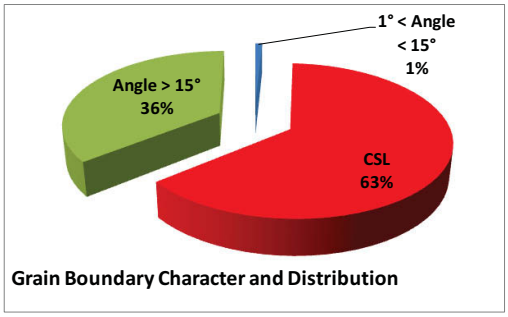

Figure 14: SiC layer grain boundary character distribution via EBSD analysis at Location 1 of the non-annealed coated particle E2.

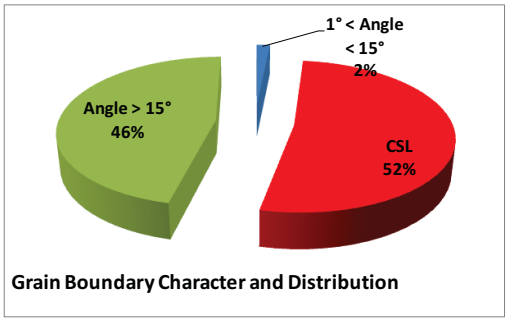

Figure 15: SiC layer grain boundary character distribution via EBSD analysis at Location 2 of the non-annealed coated particle E2.

III.B.4 Material Texture via EBSD

SiC layer texture is represented by pole figures, in which crystal orientations are plotted. Pole figures (111) corresponding to Figures 7 to 10 are shown for particles E1 and E2 in Figure 16 to 18.

From these pole figures, it can be deducted that there is no preferred orientation for the grains in the 111 direction. This work needs however to be expanded to other directions as well in future work.

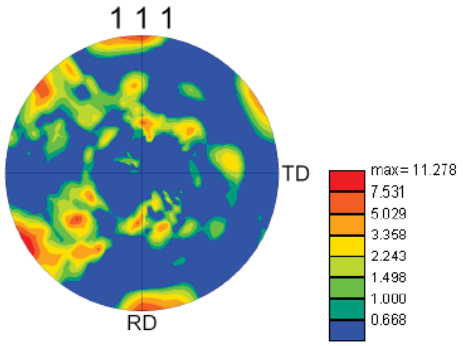

Figure 16: SiC layer crystal orientation in the 111-direction via EBSD analysis of the non-annealed coated particle E1. (TD = tangent to the surface of the particle in the plane of the cross-section and RD = normal to the plane of the cross-section)

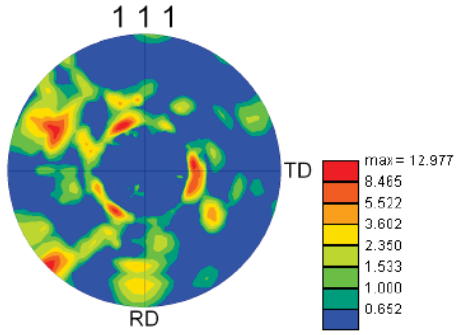

Figure 17: SiC layer crystal orientation in the 111-direction via EBSD analysis at Location 1 of the non-annealed coated particle E2. (TD = tangent to the surface of the particle in the plane of the cross-section and RD = normal to the plane of the cross-section)

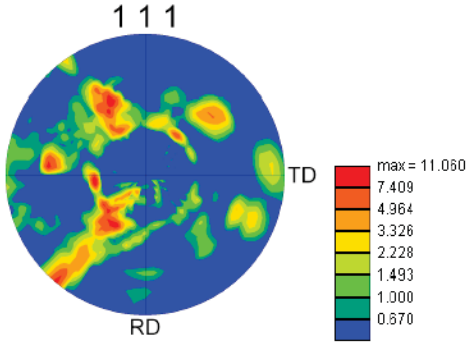

Figure 18: SiC layer crystal orientation in the 111-direction via EBSD analysis at Location 2 of the non-annealed coated particle E2. (TD = tangent to the surface of the particle in the plane of the cross-section and RD = normal to the plane of the cross-section).

III.B.5 Preliminary EBSD results of sample prepared by FIB

Preliminary results obtained from the FIB preparation technique are presented in this section. Figure 19 shows the prepared "slice" just before liftoff, showing the wedge necessary for preparation. The final FIB prepared sample ready for EBSD is shown in Figure 20. Follow-on steps include comparing these results with results obtained from a polished surface, but it was not available at the time of this paper writing.

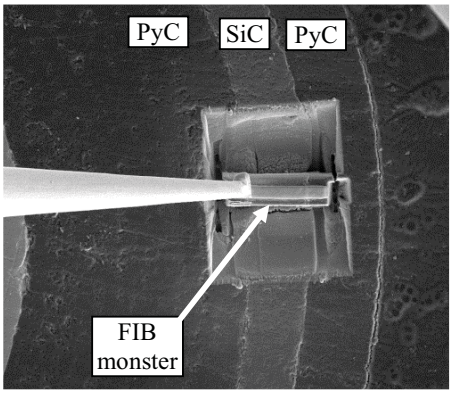

Figure 19: Micrograph showing prepared FIB slice located in the machined wedge.

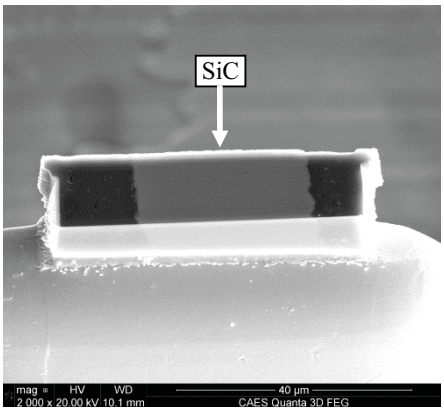

Figure 20: Micrograph showing the completed sample after final FIB machining and polishing ready for EBSD analysis.

The preliminary results are shown in Figures 21 and 22, show very small grained structure of average diameter of 0.5 µm, much smaller than found in particles E1 and E2. Although very small grained, this structure consists of a high percentage of high angle boundaries. This coated particle was fabricated in the research coater and showed typically higher strength values as compared to those of the E batch. Future work will be aimed evaluating additional particles and correlating these results with microstructural features and strength.

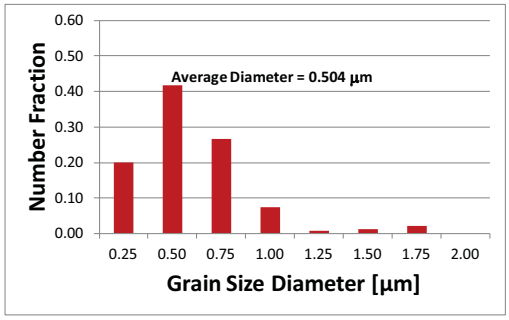

Figure 21: SiC layer grain size (diameter) distribution via EBSD analysis of FIB prepared sample of coated particle B, annealed for 100h at 1600°C.

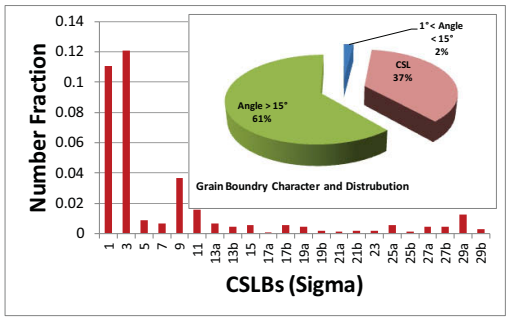

Figure 22: SiC layer grain boundary character distribution via EBSD analysis of FIB prepared sample of coated particle B, annealed for 100h at 1600°C.

III. CONCLUSIONS AND FUTURE ACTIONS

Trends seen in correlations between grain size and the two mechanical properties suggest sensitivity to the measurement techniques. It is expected that hardness and strength would vary similarly with grain size; however, the opposite trends are seen. The next step in these data analyses is to determine the theoretical (physics) relation between the two measurements and grain size.

Correlations between SiC layer hardness and strength are a function of the CVD coater. SiC layers created with the RCF coater have strengths directly related (i.e. the least squares fit line has a positive slope) to the hardness values. Correlations between the values for the three

ACF coater batches are significantly weaker and also show an indirect correlation.

Measurements of the average grain size and the grain size distribution from EBSD images proved a valuable technique that overcomes some of the shortcomings of traditional microscopic methods. Although the average grain size determined via EBSD analysis varied little among the three data sets, there does seem to be some variation in the grain boundary character distribution between these particles from a single batch and between locations on a single particle. If this preliminary observation is confirmed within more batches showing similarly variable GBCDs, the impact on coated particle characterization and qualification may be significant. No preferred orientation for the grains in the 111 direction was found. This work needs to be expanded to other directions as well in future work.

There does not appear to be any grain size difference of significance among the three data sets from Particles E1 and E2. This preliminary result may indicate SiC grain sizes among particles prepared in the same manner are sufficiently similar to allow study of fewer particles to represent an entire batch. In addition, this also may indicate that the choice of location on the cross section of a specific coated particle is not as important as there are no significant differences between the grain sizes if data sets 2 and 3. Testing this hypothesis on additional particles is recommended to improve confidence of the finding.

ACKNOWLEDGMENTS

A portion of this research was supported by the U.S. Department of Energy, Office of Nuclear Energy under DOE Idaho Operations Office Contract DE-AC07-051D14517. This work was also supported by the researchers in their private time.

Todd Morris and Tyler Czercak are acknowledged for their contributions towards the polishing techniques. Jatu Burns is acknowledged for her EBSD analysis of the FIB prepared coated particle B. The annealing of the coated particles was sponsored by PBMR as part of previous research by the authors. NMMU (Prof Jan Neethling) is thanked for the coated particles for continued research.

REFERENCES

[1] I.J. van Rooyen, J.H. Neethling and J. Mahlangu, “Influence of Temperature on the Micro- and Nanostructures of Experimental PBMR TRISO coated particles: A Comparative Study”, Proceedings of the 4th International Topical Meeting on High Temperature Reactor Technology, 28 Sept 2008 Washington DC USA, HTR 2008-58189, 2008.

[2] I.J. van Rooyen, J. Neethling, P. van Rooyen, The influence of annealing temperature on the strength of TRISO coated particles, Journal of Nuclear Materials, 402, p. 136-146, 2010.

[3] I.J. van Rooyen, J.H. Neethling, A. Henry, E. Janzen, S.M. Mokoduwe, A.J. van Vuuren, E. Olivier, Effects of Phosphorous-doping and High Temperature Annealing on CVD grown 3C SiC, Nucl. Eng. Des. (2011), doi:10.1016/j.nucengdes.2011.09.066 (In press)

[4] I.J. van Rooyen, J.J.A. Engelbrecht, A. Henry, E. Janzén, J.H. Neethling, P.M. van Rooyen “The Influence of grain size and phosphorous-doping of polycrystalline 3C-SiC on Infrared Reflectance Spectra”, Journal of Nuclear Materials, 422 (1-3), p.103-108, Mar 2012.

[5] I.J. van Rooyen, E. Nquma, J. Mahlangu and J.H. Neethling, “Nano indentation hardness measurements as a characterization technique of SiC- and pyrolitic carbon layers of experimental PBMR coated particles.” Mechanical properties and Performance of Engineering Ceramics and Composites V: Ceramic Engineering and Science Proceedings, Volume 31, Issue 2, p. 69-78 2010.

[6] ASTM E112-96 Standard Test Methods for Determining Average Grain Size, Re-approved 2004.

[7] L. Tan, T. R. Allen, J. D. Hunn, J. H. Miller, “EBSD for microstructure and property characterization of the SiC-coating in TRISO fuel particles,” Journal of Nuclear Materials, 372, p. 400-404, 2008.

[8] D. Helary, X. Bourrat, O. Dugne, G. Maveyraud, M. Perez, P. Guillermier, Second International Topical Meeting on High Temperature Reactor Technology, Beijing, China, September 22-24 Paper No: B07, 2004.

[9] V. Gupta, Regression explained in simple terms," Published by VJ Books Inc.
[10] T. Miura, K. Fujii, Koji Fukuya, K. Takashima, Influence of crystal orientation on hardness and nanoindentation deformation in ion-irradiated stainless steels J Nucl Mater 417 (2011) 984-987
[11] R. Kirchover MSc dissertation, Colorado School of Mines.
[12] ASTM E2627-10, ASTM International, U.S. 2010
[13] D. G. Brandon, Acta Metall. 14, 1479, 1966.
[14] C.S. Kim, A.D. Rollett, G.S. Rohrer, "Grain Boundary Planes: New dimensions in the Grain Boundary Character Distribution," Scripta Materialia, 54, p. 1005-1009, 2006.
[15] G.S. Rohrer, J. Li, S. Lee, A.D. Rollett, M. Groeber, M.D. Uchic, "Deriving grain boundary character distributions and relative grain boundary energies from three-dimensional EBSD data," Materials Science and Technology, 26, 6, p. 661-669, 2010.
[16] S.H. Kim, U. Erb, and K.T. Aust, "Grain boundary character distribution and intergranular corrosion behavior in high purity aluminum," Scripta Materialia, 44, p. 835-839, 2001.